# Signal Transmission in the Auditory System

**Academic and Research Staff**
Professor Dennis M. Freeman, Professor William T. Peake, Professor Thomas F. Weiss, Dr. Bertrand Delgutte

**Visiting Scientists and Research Affiliates**
Dr. John J. Rosowski, Michael E. Ravicz

**Postdoctoral Fellow**
Kenneth E. Hancock

**Graduate Students**
Alexander Aranyosi, Leonardo Cedolin, David Chen, Andrew Copeland, Amy Englehart, Roozbeh Ghaffari, Bennett Landman, Courtney C. Lane, Leonid M. Litvak, Kinuko Masaki, Martin F. McKinney, Kevin N. O'Connor, Zachary M. Smith, Betty Tsai

## 1. Middle and External Ear

**Sponsor**
National Institutes of Health (through the Massachusetts Eye and Ear Infirmary)
Grant R01 DC 00194
Grant P01 DC 00119
Grant R01 DC 04798

**Project Staff**
Professor William T. Peake, Dr. John J. Rosowski, Michael E. Ravicz, Kevin N. O'Connor

In mammals sound is coupled to the inner ear through a common set of structures, which vary in their configuration among species and individuals. Our goal is to understand the relationships between the structures and their acoustic function. This knowledge can be applied (a) to suggest the evolutionary processes that produced these structural variations, (b) to interpret the effect of pathological processes on human hearing, and (c) to guide reconstruction of damaged human ears so as to restore useful hearing.

### 1.1 Comparative Structure and Function in Mammalian Ears

We have described anatomical and acoustic features of the ears of some of the 36 species in the cat family (Felidae). From acoustic measurements in ears of 11 exotic species ranging in size from domestic cat to tiger, we have shown that acoustic behavior is related to species' size in a way that can be roughly described by shifting acoustic admittance on the frequency scale with larger animals shifted to lower frequencies. Another variable that could influence inter-species differences is habitat. To test for this possibility we focused on the sand cat (*Felis margarita*), which is about the size of a domestic cat, but inhabits only deserts in North Africa and central Asia. We were able to make acoustic measurements in a total of 16 ears of anesthetized sand cats at two zoos, and structural measurements on 6 sand cat skulls from museums. The results show that the ears of this species are unusual (compared to other species of the same size) in both structural dimensions and acoustic behavior. We have used these results to determine the advantage sand cat has, compared to domestic cat, in hearing sensitivity at "low" frequencies and have shown that the increased acoustic absorption of high-frequency sound in dry air favors the use of lower frequencies for communication. Thus, the hypothesis that the habitat could influence the frequency response of the ear is supported by these results.

In another approach to relating structure and function we have described structural variations from measurements of kitten skulls of different ages. The overall result is that the tympanic membrane and ossicles are nearly adult size at birth, whereas the air-filled cavities of the middle ear increase in size dramatically. The ossicular chain and tympanic membrane do change their spacial orientation relative to the skull during development. From these results (and some assumptions) we will predict how middle-ear signal transmission changes with age and size and how much this contributes to the improvement of hearing sensitivity that occurs during development in young cats.

### 1.2 Human Ears: Pathological and Reconstructed

Although perforations of the tympanic membrane are common and they often degrade hearing substantially, neither the key variables that influence the effect nor the mechanism(s) involved have been determined. Now two papers based on a Ph.D. thesis have clearly settled the big issues[1,2]. Measurements in human cadaver ears show that the hearing loss introduced by controlled perforations is a function of perforation size, middle ear volume and sound frequency, with the largest loss at low frequencies. The location of the perforation in the tympanic membrane is not important for small-to-moderate perforations[1]. The main features of the results are explained by a simple lumped-circuit model in which the perforation introduces a new pathway for air flow from ear canal to middle-ear cavity. The perforation is represented as a series resistance and acoustic mass whose values depend on perforation size. The primary loss-mechanism is a decrease in pressure difference across the tympanic membrane introduced by the "short circuit" introduced by the perforation[2]. A simple expression that predicts the loss for low frequencies can help clinicians' diagnoses.

A new project has begun with Dr. Saumil N. Merchant of the Massachusetts Eye and Ear Infirmary's Department of Otology and Laryngology. The goal is to test the usefulness of a laser Doppler velocimeter to measure the motion of the tympanic membrane in awake patients. Early results indicate that these measurements distinguish among some kinds of middle-ear pathology (e.g. interrupted ossicular chain versus fixation of an ossicle), which may not be separated by the usual audiometric measurements. The method also can sense differences in quality of surgical reconstructions of damaged middle ears.

## Publications

### Journal Articles, Published

S.E. Voss, J.J. Rosowski, S.N. Merchant, and W.T. Peake, "Middle-ear function with tympanic perforations. I. Measurements and mechanisms," *J. Acoust. Soc. Am*., 110: 1432-1444 (2001).

S.E. Voss, J.J. Rosowski, S.N. Merchant, and W.T. Peake, "Middle-ear function with tympanic perforations. II. A simple model," *J. Acoust. Soc. Am*., 110: 1445-1452 (2001).

### Theses

K.N. O'Connor, *Analysis of Exotic Cat Vocalizations and Middle-Ear Properties*, MEng. Thesis, Department of Electrical Engineering and Computer Science, MIT, January 2001.

[1] S.E. Voss, J.J. Rosowski, S.N. Merchant, and W.T. Peake, "Middle-ear function with tympanic perforations. I. Measurements and mechanisms," *J. Acoust. Soc. Am.*, 110: 1432-1444 (2001).
[2] S.E. Voss, J.J. Rosowski, S.N. Merchant, and W.T. Peake, "Middle-ear function with tympanic perforations. II. A simple model," *J. Acoust. Soc. Am.*, 110: 1445-1452 (2001).

## 2. Cochlear Mechanics

**Academic and Research Staff**
Professor Dennis M. Freeman, Professor Thomas F. Weiss

**Graduate Students**
Alexander Aranyosi, Andrew Copeland, David Chen, Amy Englehart, Roozbeh Ghaffari, Bennett Landman, Kinuko Masaki, Betty Tsai

### 2.1 Properties of the Tectorial Membrane

**Sponsors**
National Institutes of Health Grant R01 DC00238
W. M. Keck Foundation Career Development Professorship (Freeman)
Thomas and Gerd Perkins Professorship (Weiss)

**Project Staff**
Andrew Copeland, Amy Englehart, Roozbeh Ghaffari, Bennett Landman, Kinuko Masaki, Betty Tsai, Professor Dennis M. Freeman, Professor Thomas F. Weiss

The tectorial membrane (TM) is a gelatinous structure that lies on top of the mechanically sensitive hair bundles of sensory cells in the inner ear. From its position alone, we know that the TM must play a key role in transforming sounds into the deflections of hair bundles. But the mechanisms are not clear, largely because the TM has proved to be a difficult target of study. It is 97% water, and is therefore fragile. It is small: the whole TM would roll up and fit into little more than an inch of one human hair. Finally, it is transparent.

We have developed methods to isolate the TM so that its properties can be studied. Results using this technique (which have been reported in previous RLE Progress Reports), show that the TM behaves as a gel. The material properties of a gel are a direct consequence of its molecular architecture. Charge groups on gel macromolecules attract mobile counterions from the surrounding fluid. Thus gels concentrate ions, and thereby increase osmotic pressure. The increase in osmotic pressure induces water to move into the gel and cause it to swell. The swelling stretches the macromolecules and increases the stiffness of the gel. The important consequence is that gels have mechanical, electrical, osmotic, and chemical behaviors that are all linked by their common molecular basis.

The important parameters of a gel are the amount of fixed charge and the elasticity of the matrix of macromolecules. A simple way to estimate the bulk modulus of a connective tissue is to place it in a dynastat, apply a hydraulic pressure, and measure the change in volume. An alternative method, one more suited to the dimensions and fragility of the TM, is to apply an osmotic pressure and measure the resultant change in volume. The simplest method to increase the osmotic pressure, without changing the ionic strength of the bath solution, is to add a non-electrolyte to the bath. Some non-electrolytes (e.g., glucose) permeate the TM and, hence, do not produce a sustained osmotic pressure difference between the bath and the TM. Therefore, the TM does not shrink or swell appreciably (Figure 1). However, polyethylene glycol (PEG), with a molecular weight of 20,000, has been used effectively to increase the osmotic pressure of bath solutions for connective tissues. When 10 mmol/L of PEG is applied to the bath solution, the TM shrinks to 0.23 times its original thickness. In the two intervals in which the bath solution contains PEG, the TM has the same steady state thickness to within 1 $\mu$m. Furthermore, the shrinkage is maintained for more than 40 minutes indicating that PEG did not penetrate the TM appreciably.

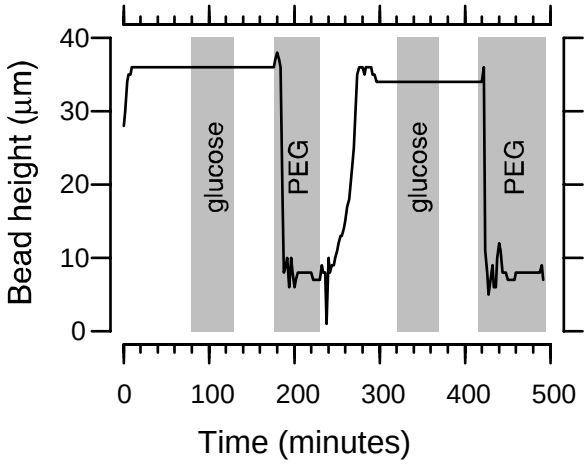


Figure 1: The height of a bead on the TM surface as a function of time as solutions of different composition are perfused through the bath. The bath solution is artificial endolymph to which either 10 mmol/L of glucose or PEG has been added in the shaded intervals.

The bulk modulus can be obtained from estimates of TM volume obtained for different concentrations of PEG and hence for different osmotic pressures (Figure 2).

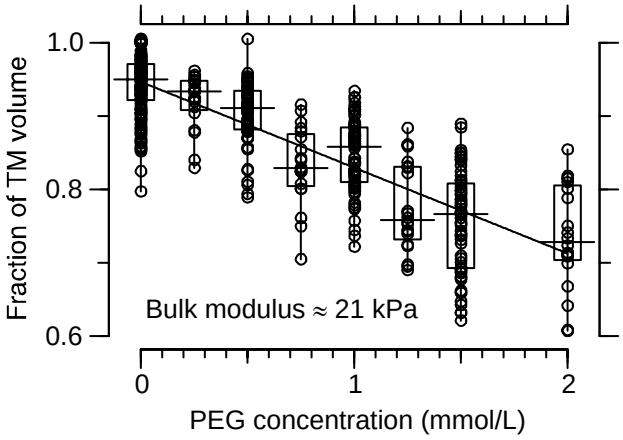


Figure 2: The fraction of the TM volume as a function of the PEG concentration of the bath solution which was artificial endolymph. A regression line was fit to these measurements. The slope of this line is inversely proportional to the bulk modulus.

The slope of the relation between the change in volume and the change in osmotic pressure is inversely proportional, through the molar gas constant and the absolute temperature, to the bulk modulus. These measurements give a value of the bulk modulus of 21 kPa.

The results of the PEG experiments can also be used to bound the fixed charge concentration as follows. Adding a small amount of PEG to the bath causes the TM to shrink roughly in proportion to PEG concentration (Figure 2). If that linear trend continued, then a concentration of 10 mmol/L would be more than enough to shrink the TM volume to zero. However, Figure 1 shows that the TM volume is reduced to only 0.23 times its normal volume. This nonlinear behavior could indicate that the mechanical constitutive relation does not obey Hooke's law and that the matrix is stiffened by compression. However, the matrix consists of a network of cross-linked elastic fibers. One might expect that the fibers could withstand tensile forces when stretched, but that they would buckle and exert little force under compression. The fibers are

normally under tension due to osmotic forces that result from charge groups attached to the fibers. When a solute that cannot permeate the TM is added to the bath, it exerts an osmotic force that reduces the tension in the fibers and shrinks the TM. Further addition of an impermeant solute will generate compression that is not resisted mechanically but is resisted electrostatically by charge repulsion.

If the bath contains equal concentrations $c_0$ of positive and negative univalent ions plus a concentration $c_I$ of an impermeant solute, then the osmotic pressure difference between the inside and outside of the TM is

$$\Delta C_\Sigma = c_+ + c_- - 2c_0 - c_I$$

where $c_+$ and $c_-$ represent the ionic concentrations in the TM. According to the gel model,

$$c_+ + c_- = 2c_0\sqrt{1+\frac{c_f^2}{4c_0^2}}\ .$$

Therefore

$$\Delta C_\Sigma = 2c_0\sqrt{1+\frac{c_f^2}{4c_0^2}} - 2c_0 - c_I\ .$$

For small $c_I$, this osmotic pressure is offset by tensile forces of mechanical origin. For large values of $c_I$, the tensile forces should be reduced to zero and further compression of the TM will concentrate the fixed charge until $\Delta C_\Sigma = 0$. Then

$$2c_0\sqrt{1+\frac{c_f^2}{4c_0^2}} = 2c_0 + c_I$$

which has a solution

$$c_f = \pm\sqrt{4c_I c_0 + c_I^2}\ .$$

For the experiment in Figure 1, $c_0$ = 174 mmol/L and $c_I$ = 10 mmol/L. Solving, we find $c_f \approx \pm 84$ mmol/L. If the amount of fixed charge is the same before and after the addition of the 10 mmol/L of PEG, then the fixed charge concentration would be $\pm 84 \times 0.23 \approx \pm 19.3$ mmol/L under normal (zero PEG) conditions.

This simple theory makes a number of assumptions. For example, we assume that PEG is completely impermeant and exerts an osmotic pressure that obeys van't Hoff's law. Furthermore, we assume that the matrix can exert tensile but not compressive forces. Despite these assumptions, it seems clear that this experiment excludes the possibility that the fixed charge concentration is greater than a small fraction of $c_0$. For example, if the fixed charge concentration were equal to half of $c_0$ normally, then it would be twice $c_0$ after compression by a factor of 4 (as in Figure 1). Changing the fixed charge concentration from $\pm 174/2$ mmol/L to $\pm 174 \times 2$ mmol/L changes $\Delta C_\Sigma$ from 17 mmol/L to 227 mmol/L. This 210 mmol/L change in osmolarity dwarfs the 10 mmol/L change in PEG concentration that caused the volume change in Figure 1. Thus, we conclude that the PEG experiment gives an estimate of the fixed charge concentration that is about $\pm 20$ mmol/L.

Based on these PEG experiments, the fixed charge concentration of the TM is approximately –20 mmol/L. This estimate is in good agreement with our previous estimates based on chemical analysis of the TM composition (-18 mmol/L) and based on experiments in which ionic strength was varied (-15 mmol/L).
This estimate of fixed charge concentration for the TM is also similar to that measured for corneal stroma (30 mmol/L). It is more than 6 times smaller than that of cartilage (-125 mmol/L), which is consistent with the fact that the dry weight of the TM is approximately an order of magnitude smaller than that of cartilage.

Based on these PEG experiments, we estimate the equilibrium bulk modulus of the TM to be on the order of 25 kPa. This is between that of intraocular lens (5 kPa) and corneal stroma (70 kPa). Thus our measurements of fixed charge concentration and bulk modulus are both physiologically plausible.

### 2.2 Sound-induced Motions of Cochlear Structures

**Sponsors**
National Institutes of Health Grant R01 DC00238
W. M. Keck Foundation Career Development Professorship (Freeman)
Thomas and Gerd Perkins Professorship (Weiss)

**Project Staff**
Alexander Aranyosi, David Chen, Professor Dennis M. Freeman, Professor Thomas F. Weiss

Mechanical vibrations caused by sound are detected by hair cells in the cochlea. The organization of hair cells and supporting cells into a tissue determines the mechanical properties of the cochlea. To better understand the mechanics of hearing, we are studying the motions of the cochlea and its component structures in response to sound stimulation. To this end, our group has developed an in vitro preparation for studying cochlear mechanics. The cochlea of an alligator lizard is clamped in an experiment chamber so that it can be viewed with a light microscope while it is stimulated with sound. By using stroboscopic illumination and the optical sectioning property of the light microscope, we obtain slow-motion, three-dimensional images of micromechanical structures during sound stimulation. We have developed image processing algorithms to make quantitative measurements of motion directly from these images with nanometer precision.

During the past year, we have used the system to investigate the mechanical properties of the hair bundles of hair cells. Hair cells are highly frequency selective mechanoreceptors. This frequency selectivity is believed to result from mechanical resonances of individual hair bundles.[3,4,5] Previous measurements of hair bundle motion provide some support for this hypothesis,[6,7] but fall short of demonstrating a mechanical resonance of hair bundles. To establish whether hair bundles are mechanically resonant, and to provide data to more thoroughly evaluate cochlear models, we have quantitatively measured the motion of individual hair bundles as a function of frequency.

Figure 1 shows the displacement of the tip and base of one hair bundle in response to a 1687 Hz tone with a pressure of 120 dB SPL in fluid (roughly 84 dB SPL at the eardrum). Displacement of the tip of the bundle lags that of the base, and is smaller in magnitude. The difference between displacement of the tip and base indicates hair bundle deflection, which is the relevant stimulus for hair cell excitation. Hair bundle deflection typically lags both displacement of the base and displacement of the tip of the bundle.

From measurements of hair bundle deflection at several frequencies we derive a micromechanical transfer function $\frac{\theta}{U_b}(f)$, where $\theta$ is the rotation of the hair bundle, and $U_b$ is the velocity of the base of the bundle. This transfer function characterizes the micromechanical stage of cochlear function. Figure 2 shows measurements of $\frac{\theta}{U_b}(f)$ for two hair bundles. The magnitudes are between 0.01 and 0.1 rad·s/cm, and typically fall with frequency at high frequencies. At low frequencies, magnitudes are typically constant or rising with frequency. The phase rolls off from at or above 0 cycles at low frequencies to -0.25 cycles at high frequencies.

---

[3] T.F. Weiss and R. Leong, "A model for signal transmission in an ear having cells with free-standing stereocilia. III. Micromechanical stage," *Hear. Res.*, 20: 157-174 (1985).
[4] D.M. Freeman and T.F. Weiss, "The role of fluid inertia in mechanical stimulation of hair cells," *Hear. Res.*, 35: 201-208 (1988).
[5] D.M. Freeman and T.F. Weiss, "Superposition of hydrodynamic forces on a hair bundle", *Hear. Res.*, 48: 1-68 (1990a-d).
[6] L.S. Frishkopf and D.J. DeRosier, "Mechanical tuning of free-standing stereociliary bundles and frequency analysis in the alligator lizard cochlea," *Hear. Res.*, 12: 393-404 (1983).
[7] T. Holton and A.J. Hudspeth, "A micromechanical contribution to cochlear tuning and tonotopic organization," *Science*, 222: 508-510 (1983).

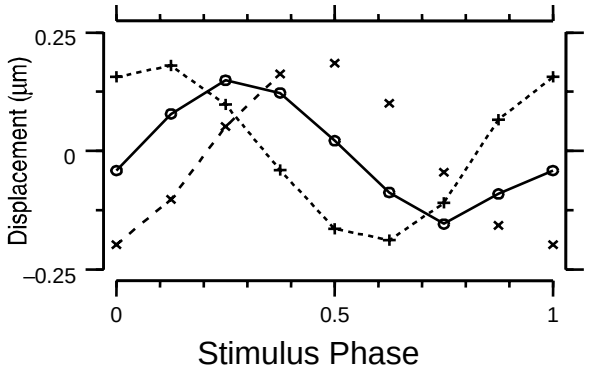


Figure 1: Motion of the tip and base of one hair bundle in response to a 1687 Hz, 120 dB SPL stimulus. The base moved by 0.191 $\mu$m peak. The tip moved 0.145 $\mu$m peak, and lagged the base by 0.190 cycles. By subtracting motion of the base from that of the tip, we get a measure of hair bundle deflection (labeled 'Tip—Base'). The hair bundle was deflected by 0.193 $\mu$m peak, and bundle deflection lagged motion of the RL by 0.377 cycles. This bundle had a height of 22 $\mu$m, so peak bundle rotation was 0.50°.

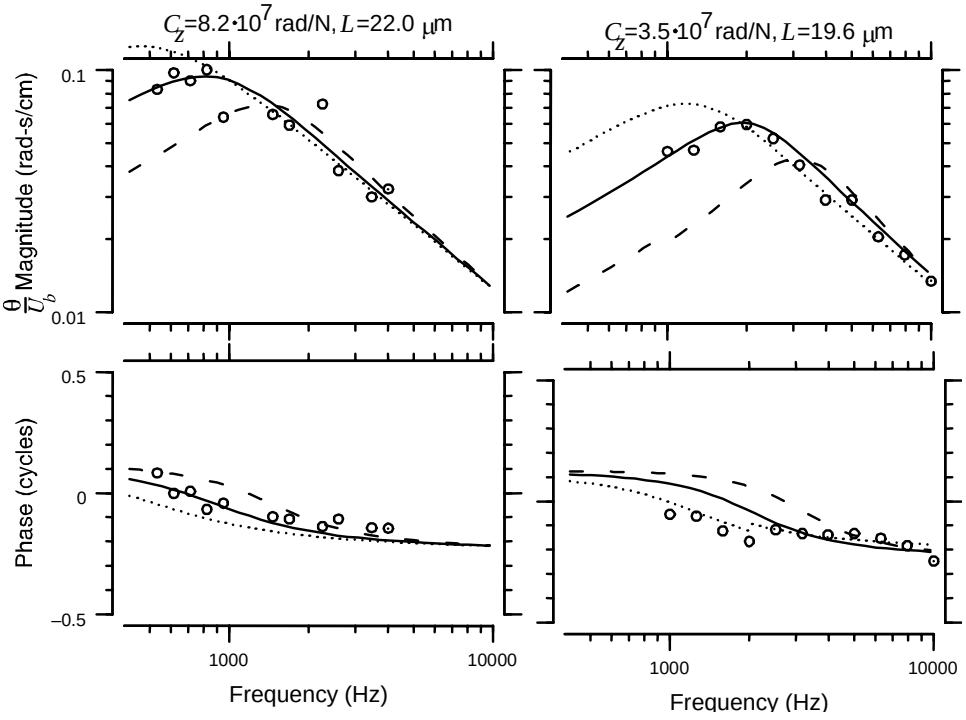


Figure 2: The micromechanical transfer function $\frac{\theta}{U_b}(f)$ vs. frequency for two hair bundles. The top plots show the magnitude of $\frac{\theta}{U_b}(f)$, the bottom plots show the phase. Circles show the measured points, solid lines are the best fits of the model of Freeman and Weiss[5] using a single free parameter $C_z$. The measured data points generally fall near the best-fit line of the model. Dotted lines show the model prediction for twice the best-fit compliance, dashed lines show predictions for half the best-fit compliance. The parameters $C_z$ and $L$ are those used in the model; $L$ is the hair bundle height as measured from images, $C_z$ is the best-fit rotational compliance of the bundle.

Figure 2 also shows the best fit of a model by Freeman and Weiss[5] to the measurements. The model describes the motion of a rigid flap attached to a moving base and immersed in water. This model has two free parameters; the height $L$ of the flap which determines the high-frequency asymptote, and the compliance $C_z$ of the attachment which determines the low-frequency asymptote. Since the heights of hair bundles were known, fits were made using only a single free parameter. The solid line on each plot shows the best fit of the model to the measurements, with the best-fit compliance $C_z$ listed above the plot. The dotted and dashed lines illustrate fits for twice and half this best value, respectively. Changing $C_z$ affects the accuracy of the fit at low frequencies, but not at high frequencies. For the subset of hair bundles for which low-frequency measurements of $\frac{\theta}{U_b}(f)$ are available, we can determine $C_z$ to within a factor of two.

From $C_z$ and $L$ we can determine the peak frequency of $\frac{\theta}{U_b}(f)$. Because some measurements of $\theta$ and $U_b$ were corrupted by ambient vibrations, we computed fits separately for all the data and for the subset of data for which motions were sinusoidal. The peak frequency $f_p$ is shown as a function of $L$ for each of these groups in Figure 3. The solid lines show the best-fit power-law relationship between $f_p$ and $L$. function of hair bundle height. Although there is significant scatter in the fits, for the tallest hair bundles $f_p$ is near 1 kHz, while for the shortest bundles, $f_p$ is near 3-10 kHz. These values are roughly comparable to the frequencies for which auditory nerve fibers innervating such cells are most sensitive.[8]

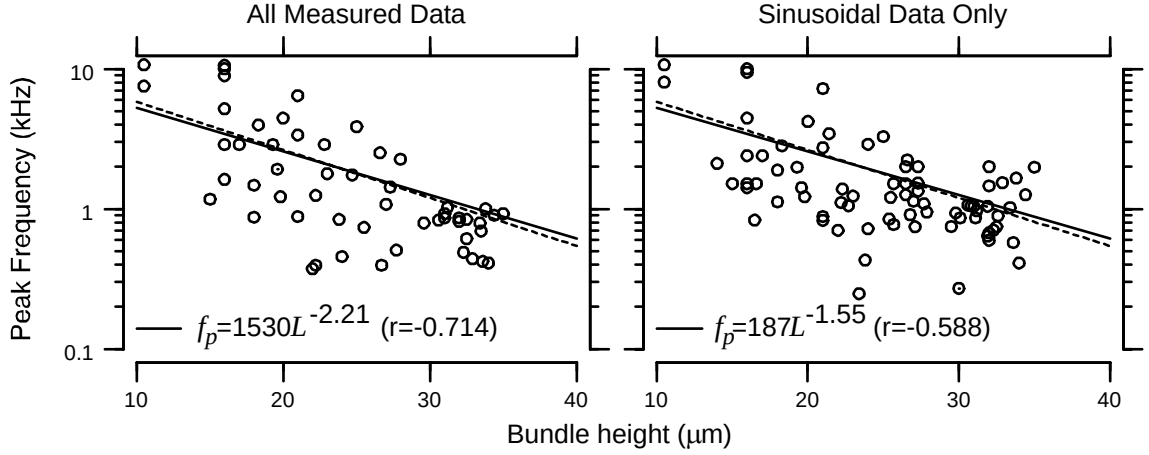


Figure 3: (cf-vs-height)Peak frequency of $\frac{\theta}{U_b}(f)$ vs. hair bundle height. The left-hand plot shows the relationship as computed for all measured data, the right-hand plot shows the relationship for the sinusoidal subset of data. Only data points for which $C_z$ was known to within a factor of two are shown. The peak frequency $f_p$ is between 500 Hz and 5 kHz for most hair bundles, and is a decreasing function of hair bundle height. Solid lines show the best-fit power-law relationship between $f_p$ and $L$, as described by the equations in the plots (with $f_p$ in kHz, $L$ in $\mu$m). The dashed line in each plot shows the relationship predicted from the phase measurements of Frishkopf and DeRosier[6], $f_p = 2.99 \cdot 10^5 L^{-1.71}$.

[8] T.F. Weiss, W.T. Peake, A. Ling, and T. Holton, "Which structures determine frequency selectivity and tonotopic organization of vertebrate cochlear nerve fibers? Evidence from the alligator lizard," in *Evoked Electrical Activity in the Auditory Nervous System*, pp. 91-112, eds. R. Naunton and C. Fernandez (New York: Academic Press, 1978).

These results provide experimental support for the model of Freeman and Weiss,[5] which shows that both viscous and inertial fluid properties play a role in cochlear function. In addition, these measurements show that free-standing hair bundles are mechanically resonant at audio frequencies, resolving a long-standing debate[9,10,5]. Our results are consistent with the hypothesis that the mechanical resonance of hair bundles determines the frequency selectivity of hair cells in the alligator lizard cochlea.

## Publications

### Meeting Papers Published

A.J. Aranyosi and D.M. Freeman, "A two-mode model of motion of the alligator lizard basilar papilla," *Abstracts of the Twenty Fifth Midwinter Research Meeting of the Association for Research in Otolaryngology*, St. Petersburg, FL, January 2002.

K. Masaki, A.D. Copeland, E.M. Johnson, R.J. Smith, and D.M. Freeman, "Measuring the equilibrium stress/strain relationship of the isolated tectorial membrane," *Abstracts of the Twenty Fifth Midwinter Research Meeting of the Association for Research in Otolaryngology*, St. Petersburg, FL, January 2002.

### Theses

B. Tsai, *Measuring the mechanical impedance of the isolated tectorial membrane*, MEng. Thesis, Department of Electrical Engineering and Computer Science, MIT, June 2001.

D. Chen, *Mechano-Electric Properties of the Lateral Line*, MEng. Thesis, Department of Electrical Engineering and Computer Science, MIT, June 2001.

B. Landman, *Broadband nanodetection using heterodyne interferometry*, MEng. Thesis, Department of Electrical Engineering and Computer Science, MIT, Feb., 2002.

[9] M. Billone and S. Raynor, "Transmission of radial shear forces to cochlear hair cells", *J. Acoust. Soc. Am.*, 54: 1143-1156 (1973).
[10] W. Bialek and A. Schweitzer, "Quantum noise and the threshold of hearing", *Phys. Rev. Lett.*, 54: 725-728 (1985).

## 3. Neural Mechanisms for Auditory Perception

**Sponsor:**
NIH-NIDCD Grants DC02258, DC00119 and DC00038

**Project Staff:**
Bertrand Delgutte, Leonardo Cedolin, Kenneth E. Hancock, Courtney C. Lane, Leonid M. Litvak, Martin F. McKinney, Zachary M. Smith

The long-term goal of our research is to understand the neural mechanisms that mediate the ability of normal-hearing people to process speech and other significant sounds in the presence of competing sounds and how these mechanisms are degraded in the hearing-impaired. In the past year, we made progress in a number of research areas including (1) the physiological basis for psychophysical frequency selectivity, (2) neural coding and perception of the temporal envelope and fine structure of sounds in both normal hearing and electric hearing through cochlear implants, (3) neural correlates of pitch and other musical percepts, (4) neural mechanisms for detection of sound signals in the presence of spatially-separated interfering sounds.

### 3.1 Frequency Selectivity of Auditory-nerve Fibers Studied with the Notched-noise Method

The notched-noise method[11] is widely used for estimating auditory filters based on psychophysical masking data. To test the physiological validity of this technique, we recorded from auditory-nerve (AN) fibers in anesthetized cats using the same stimuli as in psychophysics. Neural auditory filters derived by the notched-noise method were compared with pure-tone tuning curves measured in the same fibers.

Stimuli were pure tones in band-reject noise, with rejection bands placed both symmetrically and asymmetrically around the tone frequency. The tone was always near the fiber's characteristic frequency (CF), 10-20 dB above threshold. For each notch width, we determined the threshold noise level which just masked the increment in average rate produced by the tone. Patterson's rounded exponential filter function gave good fits to neural masked thresholds for all fibers. Both the center frequencies and the bandwidths of the fitted filters were consistent with comparable measures for pure-tone tuning curves.

We devised a neural population model based on a quantitative description of measured neural auditory filters. The population model was used to predict psychophysical detection thresholds for tones in notched noise by assuming that psychophysical threshold corresponds to the best threshold in the entire neural population. Filter models fit to the predicted psychophysical thresholds resembled the neural filter for a single fiber tuned to the signal frequency.

These results show that the notched noise method show is applicable to auditory-nerve fibers, and gives estimates of frequency selectivity broadly consistent with pure-tone tuning curves. Furthermore, the neural population model supports the assumptions underlying the notched noise method in psychophysics.

### 3.2 Relative Importance of Temporal Envelope and Fine Structure in Auditory Perception

By Fourier's theorem, signals can be decomposed into a sum of sinusoids of different frequencies. This form of analysis is especially relevant for hearing, as the inner ear performs a form of mechanical Fourier transform by mapping frequencies along the length of the cochlear partition. An alternative signal decomposition, originated by Hilbert, is to factor a signal into the product of a slowly-varying envelope and a rapidly-varying fine time structure. To investigate the relative perceptual importance of envelope and fine structure, we synthesized novel stimuli, coined "auditory chimeras", which have the envelope of one sound and the fine structure of another. We found that the envelope is most important for speech reception, while the fine structure is most important for pitch perception and lateralization based on interaural time differences (ITD). With speech, when the two features are in conflict, the sound is heard at a location

[11] R. Patterson, "Auditory filter shapes derived with noise stimuli," *J. Acoust. Soc. Am.*, 59: 640-654 (1976).

determined by the fine structure, but the words are identified according to the envelope. This finding reveals a possible acoustic basis for the hypothesized "what" and "where" pathways in the auditory cortex.

Many processing strategies for cochlear implants discard the fine time structure, and present only about 6-8 bands of envelope information. Our results suggest that modifying cochlear implant processors to deliver fine-structure information may improve patient's pitch perception and sensitivity to ITD. Better pitch perception should benefit music appreciation and help convey prosody cues in speech. Better ITD sensitivity may help the increasing number of patients with bilateral cochlear implants in taking advantage of binaural cues that normal-hearing listeners use to hear out speech among competing sound sources.

### 3.3 Physiological studies aimed at improving stimulation strategies for cochlear implants

Many modern cochlear implants use processing strategies which stimulate the cochlea with pulse trains modulated based on the input sounds. Rubinstein[12] suggested that the neural representation of the modulator might be improved by introducing a constant, high-rate, desynchronizing pulse train (DPT). A DPT may desynchronize neural responses to electric stimulation in a manner similar to spontaneous activity in a healthy ear, and thereby allow a more accurate representation of the stimulus fine structure in the temporal discharge patterns of auditory-nerve (AN) fibers. To test this hypothesis, we investigated responses of AN fibers in acutely-deafened, anesthetized cats elicited by electric pulse trains (5 kpps) delivered via an intracochlear electrode.

We had previously shown that a DPT with no modulation evokes responses in AN fibers which resemble spontaneous activity in many respects[13]. In new experiments, we recorded responses to DPTs that contained either sinusoidally modulated or vowel-modulated segments. AN fibers reliably phase locked to the modulation waveform for modulation depths as low as 0.25-1%, and dynamically changed response rate over a 20 dB range of modulation depths. For modulation depths below 5%, these fibers accurately represented the modulator waveform for both sinusoids and vowels.

These results support Rubinstein's idea that, by creating neural activity similar to spontaneous activity in a healthy auditory nerve, a DPT may lead to more natural coding of the waveform fine structure in the temporal discharge patterns of the auditory nerve. Cochlear stimulation strategies incorporating a DPT may improve pitch perception and lateralization based on ITD in implanted patients.

### 3.4 Neural Correlates of Musical Percepts

We continued our studies of neural correlates of musical percepts. Specifically, we investigated correlates of *pitch*, the essential element of melody, and *roughness*, a primary component of dissonance, in responses of single neurons in the inferior colliculus (IC) of anesthetized cats.

We had previously shown that the dissonance of pairs of diotically-presented tones forming musical intervals correlates with both the discharge rate fluctuations of all IC neurons and with average rates of the IC neurons which only respond at the onset of pure-tones[14]. In the past year, we repeated these experiments with the two tones now presented dichotically, i.e. one in each ear. We found that neurons sensitive to interaural phase differences (IPD) of pure tones showed correlates of dissonance in both dichotic and diotic conditions, while neurons insensitive to IPD only showed a correlate in the diotic condition. Furthermore, for pairs of tones forming consonant intervals, there was a correlate of the pitch of the missing fundamental in the interspike intervals of IPD sensitive neurons for both diotic and dichotic modes of presentations. To our knowledge, this is the first evidence for a neural correlate of the dichotic fusion pitch first reported by

[12] J.T. Rubenstein, B.S. Wilson, C.C. Finley, and P.J. Abbas, "Pseudospontaneous activity: stochastic independence of auditory nerve fibers with electrical stimulation," *Hear. Res*., 127: 108-118 (1999).
[13] L.M. Litvak, B. Delgutte, and D.K. Eddington, "Auditory nerve fiber responses to electric stimulation: modulated and unmodulated pulse trains," J. Acoust. Soc. Am., 110: 368-379 (2001).
[14] M.F. McKinney, M.J. Tramo, and B. Delgutte, "Neural correlates of the dissonance of musical intervals in the inferior colliculus. In *Physiological and Psychophysical Bases of Auditory Function*, D.J. Breebaart, A.J.M. Houtsma, A. Kohlrausch, V.F. Prijs, and R. Schoonhoven, Eds., Maastricht: Shaker, pp. 83-89.

Houtsma and Goldstein in 1972, which has played an important role in theories of pitch. However, the neural correlate was only convincing when the missing fundamental was below 200 Hz, while dichotic pitch can be heard up to at least 1000 Hz.

Our findings show that percepts generally considered to be high order, such as the dissonance of musical intervals, have direct correlates in neural responses in the midbrain. More generally they show that the auditory system performs processing important for music at multiple time scales.

### 3.5 Neural Correlates of the Huggins Dichotic Pitch

Dichotic pitch is a phenomenon in which changes in the interaural phase relationship of dichotically presented noise produce a tonal percept. Dichotic pitches are interesting because they can be thought of as a by-product of a binaural neural system specialized for signal detection among interfering sounds that differ in their interaural properties. One example is the Huggins pitch (HP), in which the interaural phase difference (IPD) of the noise has a given value, $\phi$, in a narrow signal band and is $\phi$-$\pi$ at all other frequencies. These stimuli produce a tonal percept at the center frequency of the band, regardless of whether the band is in phase ($\phi$=0, $HP_+$) or antiphasic ($\phi$=$\pi$, $HP_-$).

To search for neural correlates of dichotic pitch, we presented $HP_+$ and $HP_-$ stimuli to anesthetized cats and recorded the responses of delay-sensitive units in the inferior colliculus (IC). The overall interaural time difference (ITD) of each stimulus was set to the best and worst ITD of the unit, and responses were recorded as a function of signal band center frequency. The bandwidth was always 8% of the center frequency. In conditions where the signal band was positioned at a favorable ITD ($HP_+$ at the best ITD or $HP_-$ at the worst ITD), the vast majority of units showed a peak in firing rate when the band center frequency matched the unit best frequency. On the other hand, when the signal band was at an unfavorable ITD ($HP_+$ at the worst ITD or $HP_-$ at the best ITD), most units showed a notch in the firing rate when the signal band matched the best frequency. For a few units, responses were measured as a function of ITD. The majority of these showed a significant decrease in ITD sensitivity (both a drop in rate at the best ITD and an increase in rate at the worst ITD) when the signal band center frequency coincided with the neuron's best frequency. These results are consistent with an interaural cross-correlation model for delay-sensitive IC neurons, and generally support existing models of dichotic pitch.

### 3.6 Neural Correlates of Spatial Release from Masking

Normal hearing individuals have a remarkable ability to hear out sounds of interest among competing sounds. In contrast, individuals with sensorineural hearing loss have difficulty listening in noise. The goal of this research is to study the neural mechanisms of spatial release from masking (SRM), the improvement in signal detection obtained when a signal is separated in space from a masker. Two different cues seem to play a role in SRM 1) improvement in signal-to-noise ratio at one ear due to the head shadow effect and 2) detecting changes in interaural time differences (ITD) as the two sounds are separated. Here, we seek to understand the neural mechanisms used in SRM so that ultimately we may understand how these mechanisms fail as a result of damage to the auditory system.

For this purpose, we record from single units in the inferior colliculus (IC) of anesthetized cats. Our stimuli are broadband signals (100-Hz click train or 40-Hz chirp train) in a continuous broadband noise masker. Azimuths of the signal and masker are simulated by filtering waveforms through head related transfer functions. We measure each unit's masked threshold for several signal and masker azimuths.

For a vast majority of neurons, masked threshold is dependent on the masker azimuth, as it does in psychophysics. For about one-half of the high-frequency neurons, the directional dependence of masking can be accounted for by changes in signal-to-noise ratio at the contralateral ear due to the head shadow effect. These units' thresholds can be predicted by a simple model of the auditory periphery that includes a bandpass filter centered at the unit's best frequency, followed by temporal summation of the energy at the filter's output. The responses of another class of neurons tuned to low frequencies seem to be explained by their sensitivity to ITD because varying only ITD gives similar directional masking patterns as varying all of

the sound localization cues. For some of these ITD-sensitive units, the noise masker suppresses the signal response at some azimuths and saturates the response at other azimuths. This change in the form of masking can be predicted based on whether the noise azimuth corresponds to an unfavorable (suppressive) or favorable (excitatory) ITD.

Overall, the two mechanisms—detecting changes in ITD and head shadow effect—explain more than half of the unit responses we have seen. It is uncertain at this point whether other neural mechanisms, such as detecting changes in interaural level differences, may also play a role in the units' masked thresholds. Clearly, hearing impairment—which typically involves widening of cochlear filters and a loss of information at some frequencies—could severely interfere with the two neural mechanisms discussed, perhaps explaining the lack of masking release seen in hearing impaired listeners.

## Publications

### Journal Articles

#### Published

L.M. Litvak, B. Delgutte, and D.K. Eddington, D.K., "Auditory nerve fiber responses to electric stimulation: modulated and unmodulated pulse trains," *J. Acoust. Soc. Am*. 110:368-379 (2001).

M.J. Tramo, P.A. Cariani, B. Delgutte, and L.D. Braida, "Neurobiological foundations for the theory of harmony in western tonal music," *Ann. New York Acad. Sci*. 930:92-116 (2001).

#### Accepted for Publication

R.Y. Litovsky and B. Delgutte, "Neural correlates of the precedence effect in the inferior colliculus: Effect of localization cues," *J. Neurophysiol*. 87, in press.

Z.M. Smith, A.O. Oxenham, and B. Delgutte, B., "Chimaeric sounds reveal dichotomies in auditory perception," *Nature*, in press.

#### Submitted for Publication

S. Kalluri and B. Delgutte, "Mathematical models of cochlear nucleus onset neurons. I. Point neuron with many weak synaptic inputs," Submitted to *J. Comput. Neurosci*.

S. Kalluri and B. Delgutte, "Mathematical models of cochlear nucleus onset neurons. II. Model with dynamic spike-blocking state," Submitted to *J. Comput. Neurosci*.

#### Thesis

M.F. McKinney, Neural correlates of pitch and roughness: Toward the neural code for melody and harmony perception. Doctoral Dissertation, Massachusetts Institute of Technology, 2001.

### Book Chapters

S. Kalluri, and B. Delgutte, "Characteristics of cochlear nucleus onset units studied using a model," in *Computational Models of Auditory Function*, S.G. Greenberg and M.L. Slaney (eds). Amsterdam: IOS Press, pp. 29-44 (2001).

R.Y. Litovsky, C.C. Lane, C. Atencio, and B. Delgutte, B, "Physiological measures of the precedence effect and spatial release from masking in the cat inferior colliculus," in *Physiological and Psychophysical Bases of*

*Auditory Function,* D.J. Breebaart, A.J.M Houtsma, A. Kohlrausch, V.F. Prijs, and R. Schoonhoven (eds). Maastricht: Shaker, pp. 221-228 (2001).

M.F. McKinney, M.J. Tramo, and B. Delgutte, "Neural correlates of the dissonance of musical intervals in the inferior colliculus," in *Physiological and Psychophysical Bases of Auditory Function,* D.J. Breebaart, A.J.M. Houtsma, A. Kohlrausch, V.F. Prijs, and R. Schoonhoven (eds). Maastricht: Shaker, pp. 83-89 (2001).

**Abstracts**

B. Delgutte, Z.M. Smith, and A. Oxenham, "Auditory chimeras," *Abstr. Assoc. Res. Otolaryngol*. 24:623. (2001).

L.M. Litvak, B. Delgutte, and D.K. Eddington, "Responses of auditory nerve fibers to sustained electric stimulation with high frequency pulse trains," *Abstr. Assoc. Res. Otolaryngol*. 24:910. (2001).

M.F. McKinney, M.J. Tramo, and B. Delgutte. "Neural correlates of the dissonance of musical intervals in the inferior colliculus," *Abstr. Assoc. Res. Otolaryngol*. 24:191 (2001).

L.M. Litvak, Z.M. Smith, B. Delgutte, and D.K. Eddington, "Cochlear stimulation strategy that utilizes a conditioning high-frequency pulse train: single unit recordings," *Proc. Conference on Implantable Auditory Prostheses*, Asilomar, California, p. 127 (2001).

L. Cedolin and B. Delgutte, "Frequency selectivity of auditory-nerve fibers studied with band-reject noise," *Abstr. Assoc. Res. Otolaryngol.* 25:330 (2002).

K.E. Hancock and B. Delgutte, "Neural correlates of the Huggins dichotic pitch," *Abstr. Assoc. Res. Otolaryngol.* 25:153 (2002).